Chemical Engineering Journal 462 (2023) 142301

Contents lists available at ScienceDirect

Chemical Engineering Journal

journal homepage: www.elsevier.com/locate/cej

Degradation of thermoplastic cellulose acetate-based bioplastics by full-scale experimentation of industrial anaerobic digestion and composting

Giovanni Gadaleta [a,1], Sabino De Gisi [a,*], Zhi Kai Chong [b], Joern Heerenklage [b], Michele Notarnicola [a], Kerstin Kuchta [b], Livia Cafiero [c], Maria Oliviero [c,1], Andrea Sorrentino [c], Caterina Picuno [d]

[a] Department of Civil, Environmental, Land, Building Engineering and Chemistry (DICATECh), Politecnico di Bari, Via E. Orabona 4, I-70125 Bari, Italy
[b] Institute of Circular Resource Engineering and Management (CREM), Hamburg University of Technology, Blohmstraße 15, D-21079 Hamburg, Germany
[c] Institute of Polymers, Composites and Biomaterials (IPCB), National Research Council (CNR), P.le E. Fermi 1, I-80055 Portici (Naples), Italy
[d] DMTR Consulting S.r.l., Via Gennaro Guevara 5, I-70124 Bari, Italy

ARTICLE INFO

Keywords:
Composting
Dry anaerobic digestion
Full-scale investigation
Microscopic degradation
Plastics disintegration
Waste management

ABSTRACT

The ability of full-scale industrial plants to degrade bioplastics waste must be verified to exclude any negative effects on the quality of the process outputs. This study aims to assess the degradation of two thermoplastic cellulose acetate-based bioplastics, in pure and composite forms in both Anaerobic Digestion (AD) and Composting (C) industrial conditions. The main degradation occurred during AD, where a disintegration of about 36% and 50% was achieved from pure and composite thermoplastic cellulose acetate, respectively. The disintegration during C did not exceed 20% for both samples. The combined process resulted in a slightly higher degradation (58–40%) than that obtained in AD, revealing how the main alteration of samples occurred in an anaerobic environment. Despite this macroscopic degradation, the samples showed only minor superficial degradation as highlighted from SEM analysis. FT-IR spectroscopy, TGA andDSC analyses showed that the biodegradation mechanism involved mainly the plasticizer loss and deacetylation of the cellulose matrix, with only partial degradation of cellulose backbone However, both deacetylation and degradation were favored in AD and AD + C processes and from the presence of filler in anaerobic conditions. These results demonstrated how the degradation obtained on an industrial scale can differ significantly from those obtained in the laboratory scale, especially for pure thermoplastic cellulose acetate. Furthermore, current industrial AD and C process resulted not optimized for the treatment of thermoplastic cellulose acetate-based bioplastics. Hence, this works could help waste facilities managers to process emerging materials such as bioplastics in a more sustainable way.

1. Introduction

To prevent and reduce the impact of plastic wastes on the environment and to promote a transition to a Circular Economy, the European Directive for Single-Use Plastics (SUP) aims to transform radically the way plastic products are designed, produced, used and recycled in the EU [1]. For the first time, bio-based, biodegradable and compostable plastics were considered equivalent to conventional plastics under the SUP Directive. The reason for this choice was essentially due to the lack of shared technical standards to certify the actual biodegradability of these materials in real conditions, such as in the marine environment [2]. Not even the degradation of these materials under complex industrial conditions has been thoroughly documented, albeit this should be already known [3].

In this context, the term “bioplastics” is equivalently used to define either the origin (bio-based) or the fate (biodegradable) of a given plastic material. This term was introduced in the last few decades to identify a generic environmentally friendly and sustainable alternative to fossil-based materials [4]. This has produced a variegated class of commercial materials that users, distributors and consumers did not know and handle properly [5]. Despite this, the presence of bioplastics on the market is constantly growing. In 2022 the global capacity of bioplastics production of about 2.22 Mt of bioplastics was reported and it was set to increase to approximately 6.29 Mt in 2027 [6]. There is a

* Corresponding author.
E-mail address: sabino.degisi@poliba.it (S. De Gisi).
[1] These authors contribute equally to this work.

https://doi.org/10.1016/j.cej.2023.142301
Received 5 January 2023; Received in revised form 18 February 2023; Accepted 4 March 2023
Available online 9 March 2023

wide range of biopolymers such as PHA (polyhydroxyalkanoates), polylactic acid (PLA), starch-based and other that are still limited in amount but with a promising fate: it is the case of cellulose-based biopolymers, which accounted 3.6% of the global bioplastic production in 2022.

Nowadays, waste bioplastics are usually collected with the separate collected organic waste. However, it has been realized that even if bioplastics fully meet the criteria of industrial compostability (EN 13432), their treatment with separate collected organic waste through anaerobic digestion and composting must be carried out with care [7] and their general impact on the entire waste management system could not be neglected [8].

Usually, the industrial processing conditions used for the treatment of organic waste are different from that prescribed by standards, in terms of temperature, bioplastic concentration and time [9]. In addition, variable thicknesses, the presence of pollutants, additives and fillers are some of the variabilities that can affect the degradation process of a bioplastic material [10,11]. An incomplete bioplastics degradation, achieved at the end of biological treatment, results in contamination of digestate and/or compost, which must be mechanically separated in the final step (or before the biological processes) [12]. The contamination of digestate and/or compost by bioplastics fragments doesn't allow to use it in agriculture, resulting in significant environmental burden [13]. In fact, these bioplastic fragments as well as pesticide residues used in agriculture can potentially cause unpredictable damage to the environment due to their persistent bio-accumulation [14,15]. Various technologies such as bio-catalytic [16,17] and chemical treatments [18,19] have been investigated. However, most of these techniques are expensive and generate by-products that can sometimes be more toxic than the initial themselves [20,21]. Improved approaches that control plastics residues in industrial solid wastes treatments, as well as general policy measures to reduce the single-use plastics are mandatory [22].

The suitability of biological treatment for bioplastics waste has been mainly investigated by means of several laboratory tests on a wide range of biopolymers, following the process conditions established by different standard methods related to compostability, biodegradability and disintegration [23]. Concerning two thermoplastic cellulose acetate-based, a lab-scale assessment of their fate during a combined anaerobic digestion and composting process was carried out by Gadaleta et al. [24]. Results revealed a slight increase in methane production during the anaerobic digestion stage and no effect of bioplastics during composting. Despite it was not detected any phytotoxic effect of the compost with bioplastics residues, the final degradation of cellulose acetate samples did not fulfil the compost quality requirement.

On the contrary, knowledge about the real degradation of bioplastics during industrial anaerobic digestion and composting process are still scarce and limited to few biopolymers, revealing different results between full-scale and lab-scale test. Altieri et al. [25] reported that, while different Poly Butylene Succinate (PBS)–co-Adipate/Collagen Hydrolysates blend samples achieved a high degree of biodegradation at lab-scale, the samples did not fulfil the residues limit admitted for the full-scale tests. Intaraksa et al. [26] and Kale et al. [27] have reported that PLA samples are completely degraded both in the laboratory and at full-scale, but with a test duration of >90 days. In addition, both rigid and flexible packaging (PLA- and PBS-based, respectively) significantly differed in the degree of disintegration during lab-scale and on-field composting tests [28]. The rigid and flexible packaging blends achieved a disintegration of 44.3% and 99.7% after 12 weeks in the lab-scale test, respectively. After exposure to industrial composting on-field, the degradation didn't exceed 7% for both samples.

The lack of knowledge in full-scale investigation of bioplastic degradation is due to the difficulty of testing the degradability of bioplastic in full-scale reactor, that better describe bioplastic degradability than batch lab-scale conditions. In any case, most of the full-scale experimental tests present in literature considered only the composting environment, revealing the poor attention dedicated to the investigation on the anaerobic conditions. Full-scale evaluation of bioplastics degradation under anaerobic conditions was carried out only through landfill burial tests [29] or for few biopolymers such as PLA and starch-based shoppers [30]. Thus, the evaluation of bioplastics degradation at full-scale needs to be further investigated, especially in real anaerobic digestion plant, including also the case of incoming biopolymers such as cellulose-based ones.

In order to cover the gap in existing literature, this study aims to investigate the full-scale degradation of two thermoplastic cellulose acetate-based samples, in pure and composite forms (already investigated in Gadaleta et al. [24]) in both anaerobic and composting industrial conditions. The full-scale degradation experiments were carried out in a public waste treatment facility in Hamburg (DE) as an upgrade of the previous assessment in lab-scale by Gadaleta et al. [24] (which was seen as a reference test). The samples taken from the compost or digestate at the end of each degradation test are characterized by Fourier-Transform Infrared Spectroscopy (FT-IR), Thermogravimetric Analysis (TGA), Differential Scanning Calorimetry (DSC) and Scanning Electron Microscopy (SEM) to monitor and qualitatively describe the degradation mechanism at different structural scales.

2. Materials and methods

2.1. Materials

Thermoplastic Cellulose Acetate (CA) with a plasticizer content of about 30 % was supplied in form of pellets by GIBAPLAST (Varese, Italy) and used as pristine and as polymeric matrix in the obtained masterbatch and composite. Cellulose acetate (39.8 wt% acetyl content, degree of substitution (DS) 2.5, specific gravity ~ 1.31 and average molecular weight Mn ~ 50,000) and Triacetin (99.5% purity, molecular weight Mw ~ 218.2 g/mol) were used by GIBAPLAST to prepare CA.

A layered double hydroxide (LDH) intercalated with sorbate anion, listed in EC-Directive 10/2011 was used as active nanofiller. It was produced by Nicefiller Ltd., a startup of the University of Salerno (Italy) [31]. The active molecule in the nanofiller is equal to 20 wt% (wt%).

2.2. Thermoplastic cellulose acetate-based bioplastics preparation

Two different CA based bioplastics, in pristine and composite form, were prepared. A composite of CA with 5 wt% of organically modified LDH was prepared in two steps. Initial step involved the preparation of a masterbatch to obtain a good dispersion of filler in the polymeric matrix. Masterbatch was prepared by mixing 45 g of CA with 25 g of organically modified LDH in an internal mixer (Rheomix 600 Haake, Germany), at 140 °C and 75 rpm. Before the mixing process, CA was dried in a laboratory oven at temperature 80 °C for 8 h. Preparation of the masterbatch in the mixer was carried out in two stages. In the first, CA was melted for 2 min; in the second, LDH was added and the mixture was stirred for 3 min. Subsequently, the composite containing 5% of organically modified LDH was extruded using 430 g of pristine CA with 75 g of masterbatch. The extrusion process was carried out using a twin-screw extruder (Thermo Scientific 121 EuroLab 16 XL) at 40 rpm and temperature profile: 150 °C, 160 °C, 160 °C, 160 °C, 160 °C, 160 °C, 150 °C (head) to form a continuous, 150 μm thick, film samples (namely CA-LDH). Before extrusion, CA and masterbatch were dried in a dryer for 8 h at 80 °C. Pristine thermoplastic cellulose acetate film samples (namely CA) were produced by applying the same procedure to the CA pellets.

2.3. Anaerobic and composting facility

The facility used for the full-scale experiments is Biogas-und Kompostwerk Bützberg, located in Hamburg (BKW Bützberg, SRH), which has a typical layout of a combined anaerobic and composting plant in Europe [32] (Fig. 1a).

It is a public waste treatment utility of the city, producing biogas as

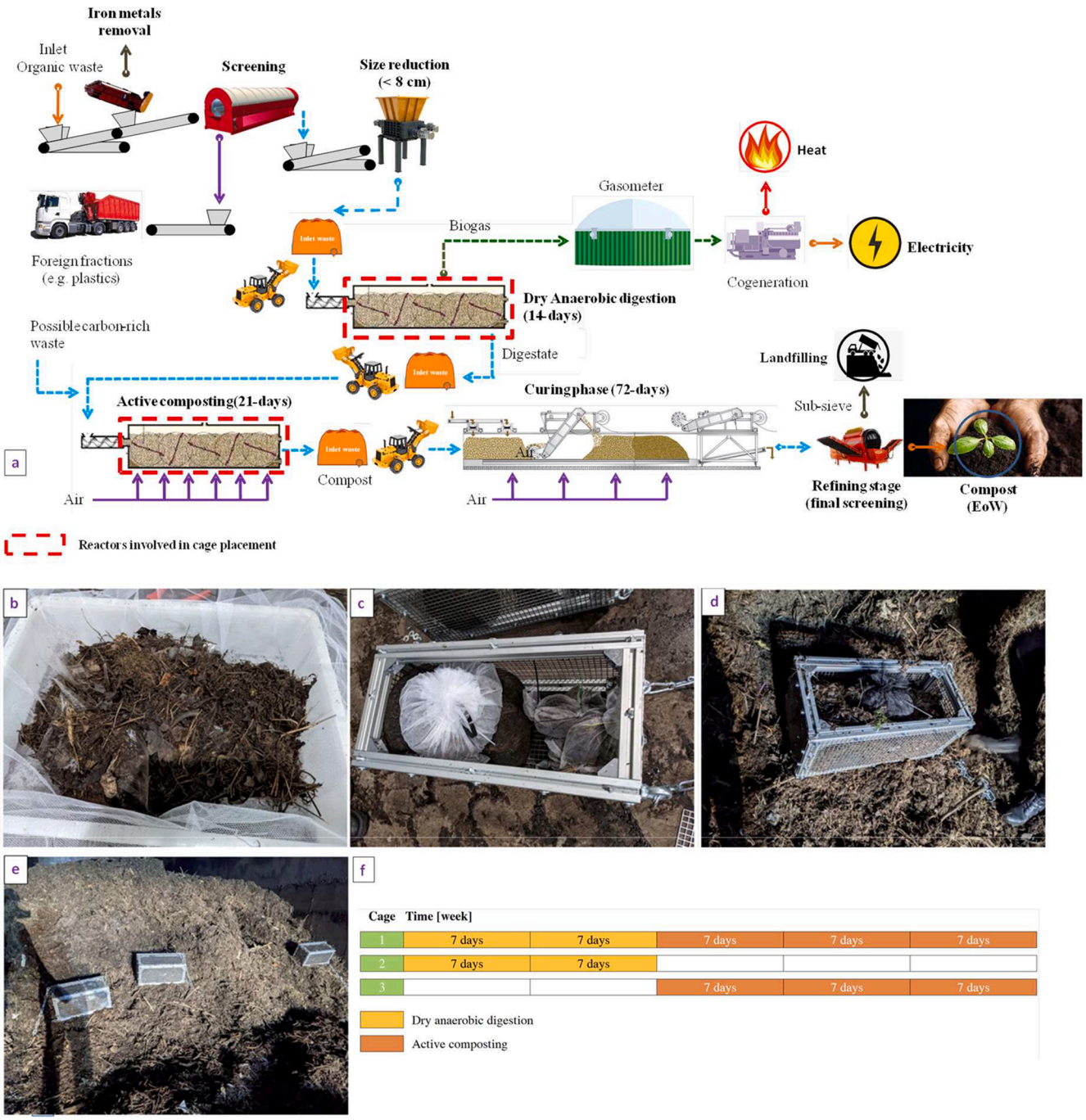

Fig. 1. Full-scale plant layout with reactors involved in cage placement (a); Cages preparation and positioning: (b) mixture of CA based samples with separate collected biowaste/digestate, (c) placing the net in the metal cage, (d-e) placing the cages in the biomass to process and covering them; Experimentation timeline (f). Single images with higher resolution are shown in Supplementary Materials.

well as compost via dry-anaerobic digestion (solids content >20%) and composting from organic waste. The facility has a capacity of 70,000 Mg of bio-waste and it can produce annually 1.3 million m^3 of bio-methane and 35,000 Mg of compost [33]. The waste is collected, sieved to remove impurities (e.g. plastic films or metals) and then shredded with an average dimension of 8 cm through a screw mill crusher. Then, about 150 Mg of organic waste (80% of raw material from bio-waste, 5% of structure from green waste, 10% of digestate and 5% of processed sieve overflow) are fed to one of the 21 box-shaped fermenters (24 m × 5 m × 4.5 m) and 2–3 weeks of mesophilic anaerobic digestion (38–40 °C) with leachate percolation are carried out. Biogas is collected and purified to reach high methane concentration and used for the Hamburg energy supply. The digestate in output is then mixed with raw bio-waste as process initiator and fed into a box-shaped reactor (22 m × 125 m): there for 4–5 weeks the digestate is aerated (6 times per hour) held at 60 °C and every 7 days it is mixed and moisturized. After composting, the finished compost is sieved and made available for marketing. Over-screens (>10 mm) are removed through a wind sifter and reused as structural material while impurities removed at the beginning of the process (1.5 – 2.5 % of the input) are incinerated.

2.4. Samples preparation and experimental degradation tests

In order to evaluate bioplastic degradation during biological

treatment, (i) anaerobic digestion (AD), (ii) composting (C) and (iii) combined anaerobic digestion and composting (AD + C) have been carried out on both CA and CA-LDH samples. The waste loading of the anaerobic digestion fermenter was 145 Mg of organic waste, in which, due to the waste composition fluctuation, no green waste was added.

CA and CA-LDH film samples were cut in pieces of 100 cm^2 surface and placed into plastic nets of 2 mm mesh, as established by normative EN ISO 16929:2021 [34]. Indeed, a bioplastic can be considered disintegrated when the size of the residues is under 2 mm and inert materials (i.e., plastic, glass, metal, and bioplastic) with a size under 2 mm are not considered to negatively affect the quality of fertilizers. For each environment (AD, C and AD + C), three nets (triplicate) were prepared for both CA and CA-LDH samples, in order to overcome the problem associated with the complexity of full-scale study. Every net contained about 1 kg of bio-waste (items with a dimension >50 mm were manually removed) and a specific number of plastic samples (from 8 to 14) were added in order to achieve 1 % of bio-waste (wet mass basis). All the nets were placed in a specific cage (25 cm × 25 cm × 51 cm) for each environment (AD, C and AD + C) with a metal grid of 3 cm × 3 cm, allowing a continuous contact with the rest of the pile and protecting the nets for possible damage (Fig. 1b–1e). The cages were placed in the middle of the bio-waste pile and properly marked [35]. As visible in Fig. 1e, three cages were used: two of them were placed in the anaerobic digestion fermenter at the same moment. At the end of the process, the first was opened to assess the plastic degradation and the second one was transferred to the composting unit to assess the whole anaerobic–aerobic treatment. A third cage was introduced in the same composting stage to assess the plastics' aerobic degradation only. AD was conducted for 15 days while active C was conducted for a further 21 days (with weekly mixing) (Fig. 1f). The reactor adopted was the same, equipped to work under anaerobic (no aeration) and aerobic conditions.

2.5. Analytical methods

In order to characterize the CA based waste with regard its physical, morphological and chemical properties, different analytical methods were applied, herein presented.

2.5.1. Total and Volatile solids, elementary composition, electrical conductivity, pH

Total solids (TS) and Volatile solids (VS) were determined by following DIN 38414 – S2 [36] and DIN 38409 – H 1–3 [37], respectively. pH was measured for both liquid and solid samples: for the latter, the DIN 38404 – C5 [38] was adopted. The elementary composition of the output from the different stages of composting was evaluated using an NCHS analyser (Vario MACRO cube, Elementar). Electrical conductivity was measured for the final compost in accordance with the DIN 38404 – C8 standard [39].

2.5.2. Plastic disintegration

Plastics disintegration was evaluated at the end of every stage: (i) after 2 weeks for AD, (ii) after 3 weeks for C and (iii) after 5 weeks for AD + C. At the end of each process, the nets were opened, the material was dried at 105 °C and then sieved. Plastic samples with dimension >2 mm were recovered, manually cleaned from macroscopic impurities and weighed. According to ISO 16929, the degree of disintegration (D) was calculated from the Eq. (1):

$$D = \frac{(m_i - m_r)}{m_i} \times 100 \quad (1)$$

where m_i is the initial dry mass of the test material and m_r is the dry mass of the residual test material recovered by sieving (2 mm). Although the ISO 16929 standard refers to the aerobic environment, for comparison purpose, here the calculation of the degree of disintegration was also extended to the anaerobic environment.

2.5.3. Scanning Electron Microscopy (SEM)

SEM X Carl Zeiss Sigma 300 VP (Carl Zeiss Microscopy GmbH, Jena, Germany) was used to characterize the surface morphology of the samples before and after degradation. Before placing the samples in the vacuum chamber, they were coated with graphite by using Sputter Quorum Q150 (Quorum Technologies Ltd., East Sussex, UK). The images were captured using an acceleration voltage of 5 kV at a working distance of 6–9 mm.

2.5.4. Thermogravimetric analysis (TGA)

A thermogravimetric balance, TGA Q500 (TA Instruments, USA), was used to analyse the thermal degradation behaviour of the test samples between 30 °C and 800 °C at a heating rate of 10 °C/min in a nitrogen atmosphere.

2.5.5. Differential Scanning colorimetry (DSC)

A DSC Discovery differential scanning calorimeter (TA Instruments, USA) was employed to determine the change in glass transition temperature (T_g) after the degradation process. The samples were weighed and analysed under a nitrogen atmosphere at a heating rate of 10 °C/min from −50 to 200 °C.

2.5.6. Fourier transform Infrared spectroscopy (FT-IR)

FT-IR analyses were performed using a Nicolet apparatus (Thermo Scientific, Italy) at ambient temperature. The samples were analysed in ATR spectra mode from 4000 to 600 cm^{-1} with a wavenumber resolution of 4 cm^{-1} for 64 scans. These analyses were performed before and after degradation.

3. Results and discussion

3.1. Anaerobic digestion and composting output

The main bio-waste characteristics evaluated at the end of each treatment step are summarized in Table 1.

It is possible to note that, during the AD step, the water content in the bio-waste increased due to leachate recirculation. Once C started, the bio-drying that characterizes that process was responsible for a rise in TS. On the opposite, during the AD treatment a significant reduction of VS, electrical conductivity and C/N was observed. This increase proceeded slower in the following C process. All parameters presented here were comparable with that measured during the lab-scale degradation of the same materials, confirming the effectiveness of the full-scale process. During the AD step, the biomass reached an average temperature of 41 °C. Instead, the C process was characterized by an average temperature of 64 °C. In particular, Fig. 2 shows the temperature variation over the course of 22-days of composting process assessment.

Every 7 days, the mechanical mixing of the material caused a sharp drop in temperature to a minimum of 35 °C. The temperature during the C process varied between 45 and 70 °C with a peak up to 78 °C during the second week of processing.

3.2. Plastics disintegration

Fig. 3 shows the disintegration degree of CA and CA-LDH samples

Table 1
Changes of TS, VS, pH, electrical conductivity and C/N during AD and C.

Treatment step[(a)]	TS [%]	VS [%TS]	pH [-]	Conductivity [mS/cm]	C/N [-]
AD input	49.7	53.8	5.48	2.49	25.44
AD output	37.1	37.77	6.77	2.00	18.84
C day 14 (turning)	43.1	38.4	6.81	1.94	–
C output	47.6	40.5	6.74	1.87	17.63

[(a)] : AD = Anaerobic digestion; C = Composting.

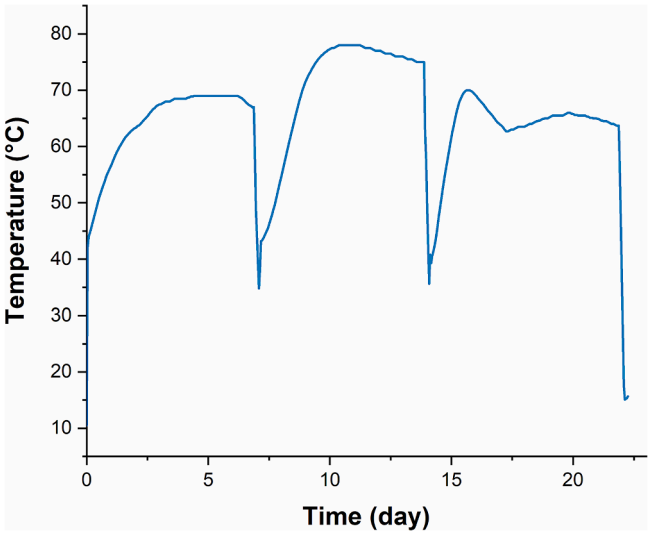

Fig. 2. Temperature changes of the composting fermenter during the C disintegration test.

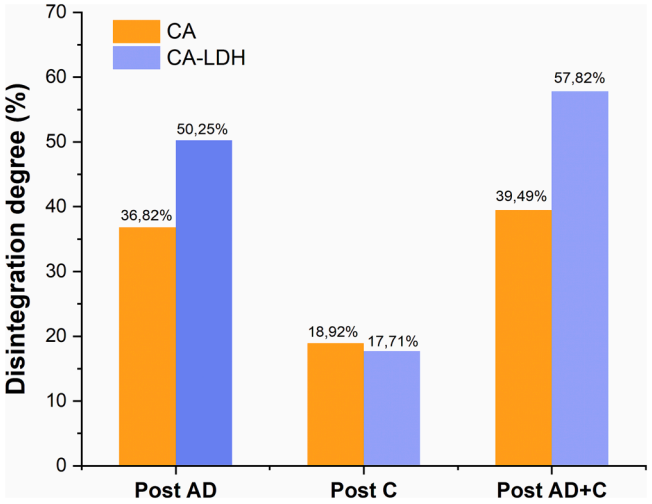

Fig. 3. Degree of disintegration (%) of CA and CA-LDH samples after AD, C and AD + C.

evaluated after each degradation step.

It is possible to note that the lowest degree of disintegration was achieved at the end of the C process where the CA and CA-LDH samples resulted in comparable values: 18.92 % and 17.71 %, respectively. At the end of the AD process, higher levels of disintegration were achieved for both CA and CA-LDH samples. In particular, CA showed a lower disintegration (36.82 %) than CA-LDH (50.25 %). In this case, the presence of LDH filler in the CA matrix seemed to promote its disintegration. The combination of AD and C processes produced a similar degree of disintegration: 57.82 % for CA-LDH and 39.49 % for CA samples. These values were comparable to the ones reached after AD, confirming the minor degradation that occurred under aerobic environment.

The lower level of disintegration of the CA samples with respect to that of CA-LDH under anaerobic environment was not in agreement with that founded on the same materials at lab-scale [24]. This discrepancy was probably due to the difference in anaerobic environment between industrial and laboratory scale. The first was conducted at solid-state condition, instead the latter at liquid-state. In addition, the scale-up could have influenced the overall degradation as well, as already pointed out for the anaerobic digestion of cellulose acetate [40]. In addition, CA disintegration was positively influenced by the presence of water in the anaerobic environment. On the other hand, the presence of water did not affect aerobic degradation, which was quite slow for CA [41]. Indeed, the aerobic degradation achieved similar values between industrial and laboratory scales, despite the moisture level being significantly different (52.4% and 38.7% for industrial and laboratory scales, respectively).

It is important to note that the disintegration values obtained at full scale were referred to a mesophilic temperature (40 °C). The adoption of thermophilic temperature might increase the methane production from the organic waste but also the bioplastic waste degradation. Indeed, it is reported how the biodegradation time necessary for most of the biopolymers (e.g PLA, starch-based) was reduced when AD was performed under thermophilic instead of mesophilic conditions [42,43]. Changes in the mechanical properties of bioplastics (for PLA, reaching its glass transition temperature) can occur only under thermophilic conditions, making them more hydrophilic and accessible for microbial hydrolysis [44].

The visual characterization of the samples before and after each degradation step allows interesting observation of the process (Fig. 4). Single images with higher resolution are shown in Supplementary Materials.

After the C process, both CA and CA-LDH samples retained their initial shape and do not present any sign of degradation caused by the contact with the substrate. After the AD process, the degradation was more evident for both samples. The surface of the CA samples showed deep cracks and holes, whereas the CA-LDH samples presented only small damages, mainly on the border. In any case, the lack of fragments in the nets allowed the conclusion that both specimens held their initial shape during the process. After the combination of AD and C process, the surface of the samples showed a level of damage similar to that occurred after only AD. However, in this case, a significant number of fragments was recovered from the nets. It was probably due to the longer time in contact with the bio-waste.

3.3. SEM analysis

Fig. 5 shows the morphology evolution of CA (1) and CA-LDH (2) samples before and after the degradation processes. In Fig. 5.1a and 5.2a, the morphology of the pristine CA and CA-LDH samples presented a smooth-surface. Single images with higher resolution are shown in Supplementary Materials.

AD caused a well-distributed surface degradation on both CA (Fig. 5.1b) and CA-LDH (Fig. 5.2b) samples. In particular, CA-LDH samples revealed a more evident degradation as confirmed by the higher degree of disintegration (see Fig. 3). For this sample, exfoliation, cracks and some fractures of the surface could be detected even at lower magnification. A higher degradation degree of the sample is responsible of significant embrittlement of the material with a consequent production of fractures on the surface. SEM images of CA and CA-LDH samples after C (Fig. 5.1c and 5.2c) did not show relevant signs of degradation. On these samples, SEM images only evidenced punctual and superficial scrapes, which were probably caused by mechanical stresses during aeration processes. The presence of a fracture in the SEM images of CA sample after C process can be due, instead, to the plasticizer leaching from a portion of film richer of triacetin. As expected, the combination of AD and C emphasized the surface damage of both samples (Fig. 5.1d and 5.2d). The superficial roughness increased, with some hints of holes due to the activity of microorganisms. Also in this case, the highest level of damage was reached by CA-LDH samples, where signs of degradation could be detected also at lower magnification. The chemical analysis of CA-LDH samples revealed a significant presence of calcium, attributed to contamination of the organic waste during the process. In general, the degradation patterns for the tested samples were comparable to that registered on LDPE samples investigated in similar conditions by

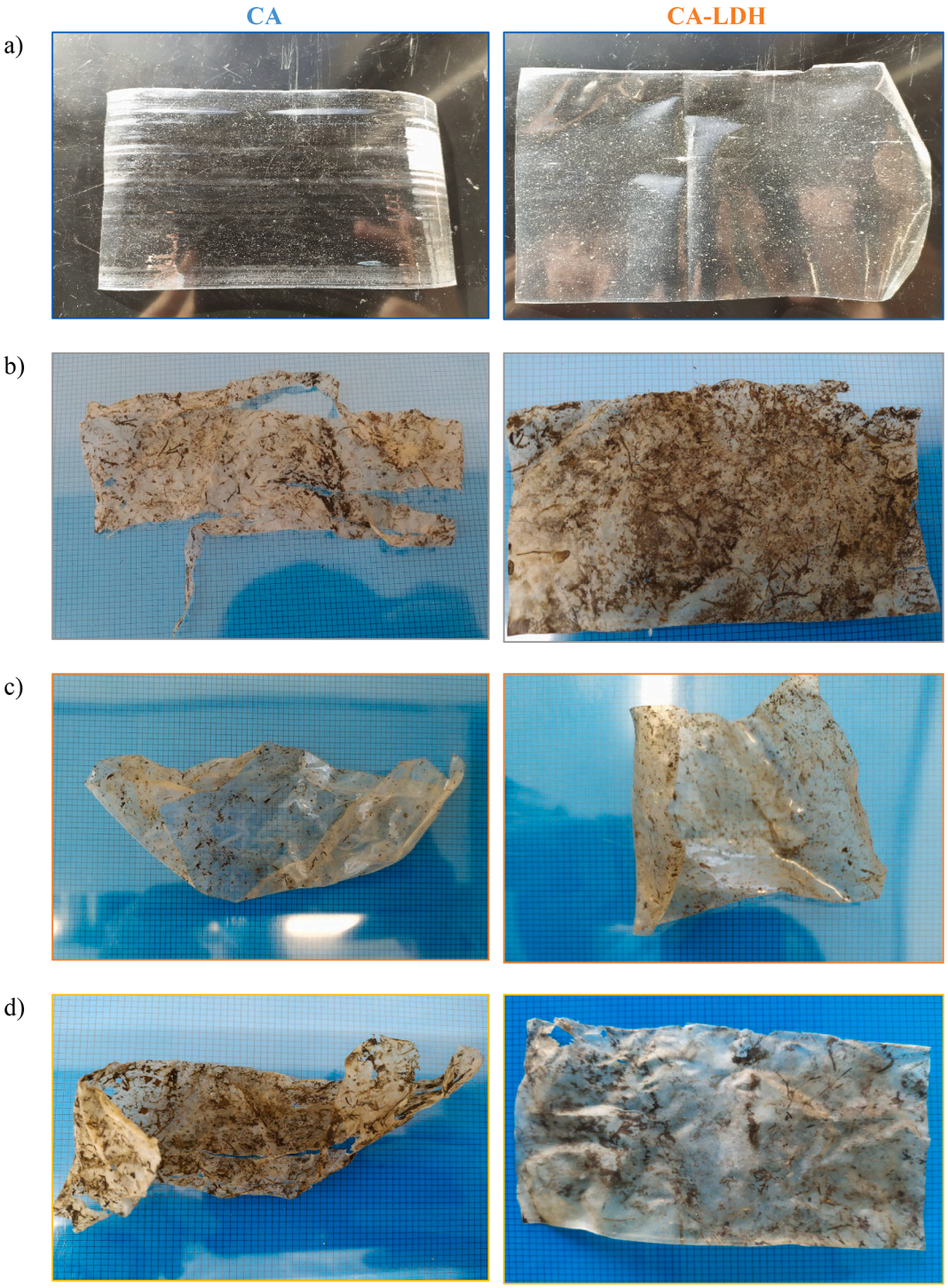

Fig. 4. Visual inspection of CA and CA-LDH samples before treatment (a), post AD (b), post C (c) and post AD + C (d).

Alassali et al. [45].

3.4. Thermal analysis

TGA curves of the CA and CA-LDH samples before and after C, AD and AD + C processes are reported in Fig. 6a and 6b, respectively (single images with higher resolution are shown in Supplementary Materials). The main thermal parameters recovered by the analysis of these weight loss curves are summarized in Table 2. These curves clearly show that the thermal decomposition of the pristine CA and CA-LDH occurred in three successive steps: evaporation of moisture, plasticizer evaporation and thermal pyrolysis of the cellulose acetate backbone [46]. The plasticizer evaporation in both samples occurred at higher temperatures (220 °C for CA and 228 °C for CA-LDH) with respect to that of the sole plasticizer (190 °C) [47] for its interaction with cellulose acetate molecules.

The initial thermal degradation temperatures (T_I) for the CA and CA-LDH samples were 316 and 297 °C, respectively (Table 2). In the same Table 2, the temperature at maximum degradation rate is also reported, denoted as T_{max}. After different degradation processes, the step of moisture loss became more evident for the increase of absorbed water from the sample during the degradation processes, while the step of

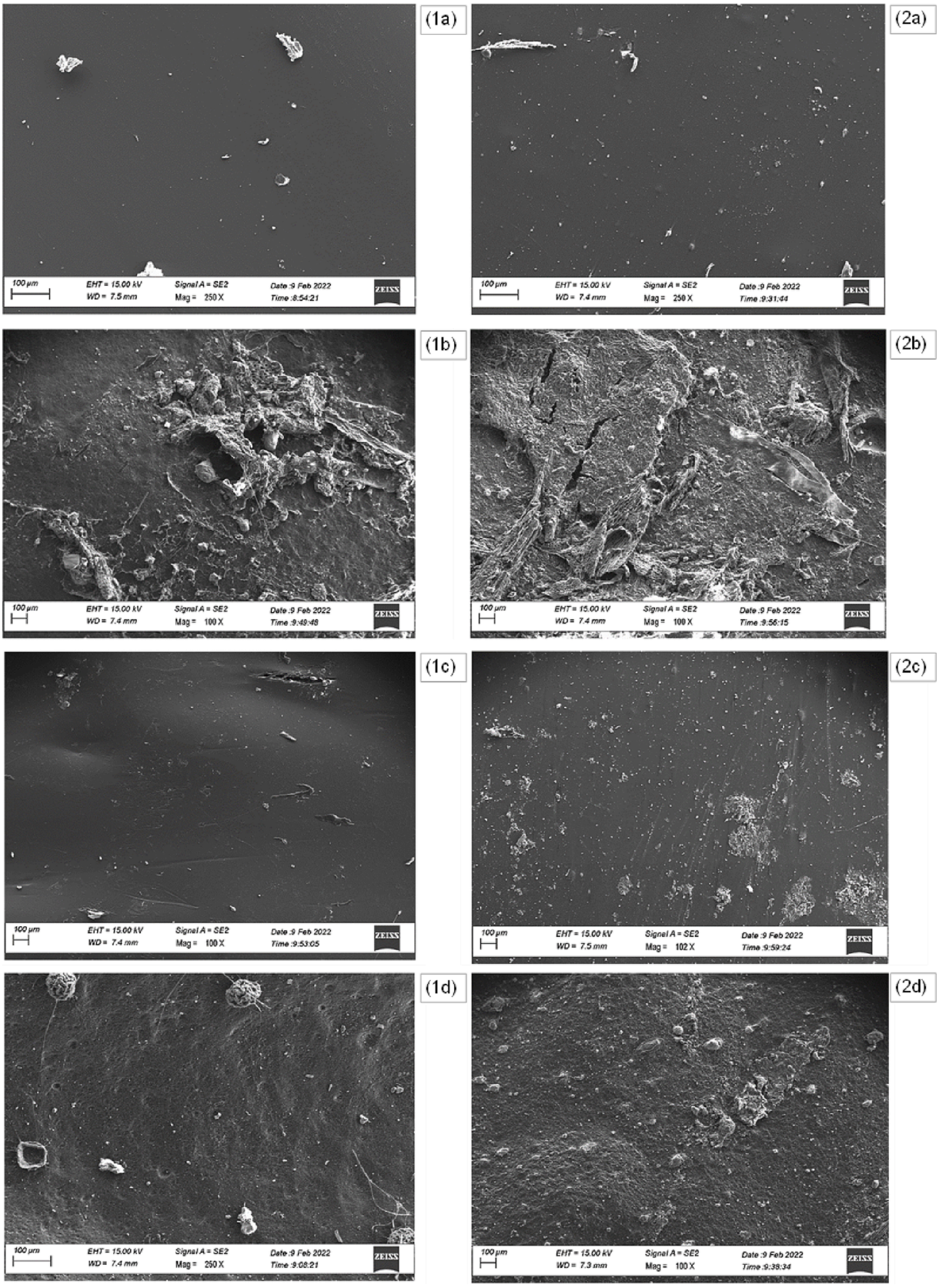

Fig. 5. SEM images of (1) CA and (2) CA-LDH samples at different stages: (a) before biodegradation; (b) post AD; (c) post C; (d) post AD + C.

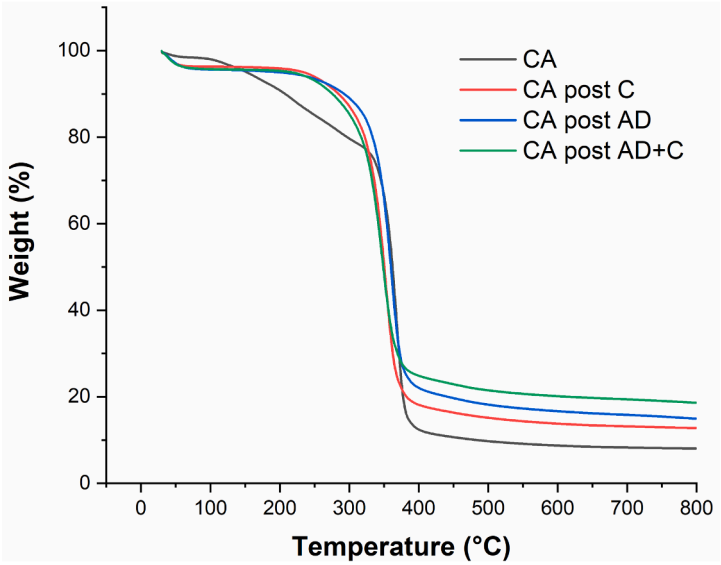

(a)

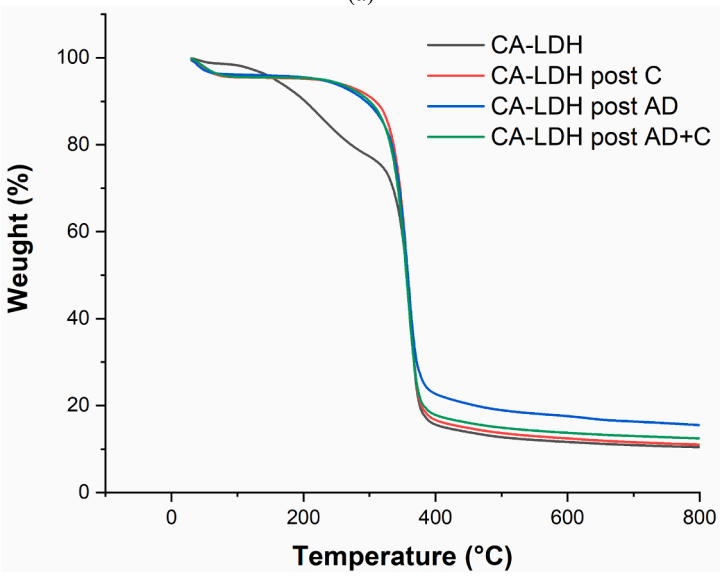

(b)

Fig. 6. TGA curves for (a) CA and (b) CA- LDH before and after C, AD and AD + C.

Table 2
TGA and DSC results for CA and CA-LDH samples before and post C, AD and AD + C.

Sample	T_{TA} (°C)	T_I (°C)	T_{max} (°C)	Residue (%)	T_g (°C)
CA	220	316	369	9	127
CA post C	–	207	360	13	195
CA post AD	–	205	353	15	192
CA post AD + C	–	195	348	19	198
CA-LDH	228	297	362	11	115
CA-LDH post C	–	230	360	11	194
CA-LDH post AD	–	208	358	16	192
CA-LDH post AD + C	–	205	356	13	197

plasticizer evaporation disappeared, indicating the complete loss of plasticizer from CA and CA-LDH samples. The thermal stability of both CA and CA-LDH samples reduced post degradation processes; in particular, T_I was significantly lowered in comparison with T_{max} and post AD and AD + C processes, for which a higher degradation degree was evaluated. Finally, it was also noticed that after C, AD and AD + C the thermal degradation residue of CA and CA-LDH increased. This increase could be due to the inorganic component of the compost/digestate in which the test samples were incubated [48].

Fig. 7a and 7b show the DSC heating curves of the CA and CA-LDH samples, respectively, before and after C, AD and AD + C processes (single images with higher resolution are shown in Supplementary Materials). The corresponding glass transition temperatures (T_g), determined as the onset of the DSC signal from the baseline shift, are summarized in Table 2.

Normally, a polymeric material subjected to biodegradation shows a strong reduction in T_g due to the decreased molecular weight and the increased mobility of the molecular chains plasticized by water molecules [49]. On the contrary, the thermograms in Fig. 7 show that for all the analyzed samples, the T_g resulted increased after the degradation processes. This was probably connected to plasticizer leaching and to the deacetylation process that leading to an increased hydrogen bonding with partial regeneration of the cellulose structure [50]. The thermal results highlighted that both phenomena are more significant with respect to the molecular weight reduction normally induced by the degradation processes.

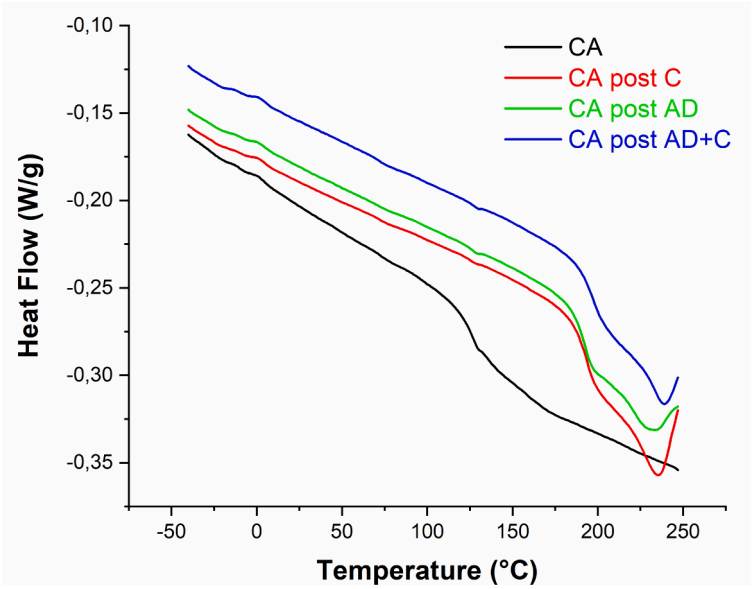

(a)

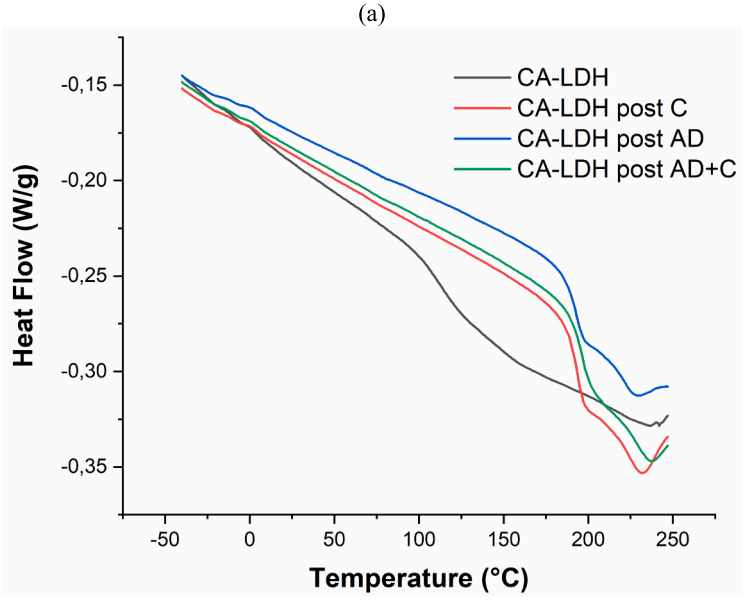

(b)

Fig. 7. DSC curves for (a) CA and (b) CA- LDH before and after C, AD and AD + C.

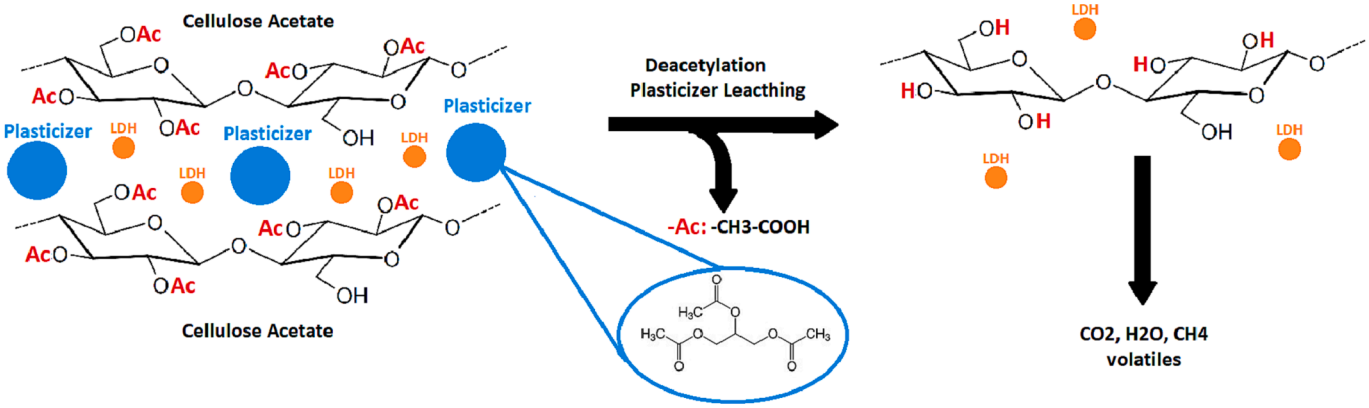

Fig. 8. Potential degradation pathway of CA and CA-LDH samples.

As previously reported in literature [51], in parallel to the plasticizer leaching, the key mechanism for the degradation of CA and CA-LDH samples was an initial deacetylation step, mediated by chemical hydrolysis and acetylesterase. Only after complete or partial deacetylation, the degradation could proceed by scissions of "regenerated" cellulosic chains, named intermediate metabolites, by enzymes including cellobiohydrolases and cellobiases, which shortened the chain length and led to weakened and embrittled material and finally to production of sugars, named end metabolites [52]. The potential degradation pathway of samples is reported in Fig. 8.

Cellulose acetate acetylation and chain scission is possible through the action of acetyl esterase enzymes and enzymes including cellobiohydrolases and cellobiases, respectively [53]. Acetyl esterases are enzymes produced by many microorganisms: *Trichoderma reesei*, *Schizophyllum commune*, *Aspergillus awamori*, *A. niger*, *A. oryzae*, *A. japonicus*, *Termitomyces clypeatus*, *Coriolus versicolor*, *Fibrobacter succinogenes*, *Thermomonospora fusca* and *Bacillus pumilus* [54]. The cellulases are, instead, a class of enzymes, produced mainly by cellulolytic fungi and bacteria, that catalyze hydrolysis of the β-1,4-glucosidic bonds that link the glucosyl units of cellulose [55]. On the other hand, the presence in the organic waste of such microorganisms or any other actually responsible of cellulose acetate degradation were not investigated by this work.

3.5. FT-IR spectroscopy

A further characterization of the chemical changes occurred by the samples during the different degradation processes is obtained by ATR-FTIR spectroscopy. Fig. 9a and 9b show ATR spectra of CA and CA-LDH samples before and after C, AD and AD + C processes, respectively. Single images with higher resolution are shown in Supplementary Materials.

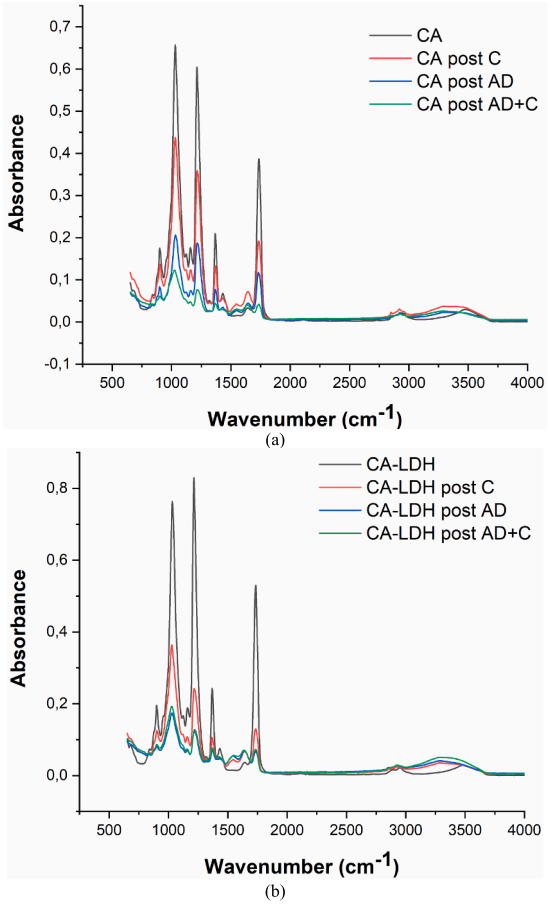

Fig. 9. FT-IR spectra before treatment and post AD, C and AD + C of (a) CA samples; and (b) CA-LDH samples.

The CA and CA-LDH samples before degradation exhibited a broad peak at 3483 cm^{-1} assigned to the –OH stretching of unacetylated cellulose. The absorption peaks at wavenumber of 2947 and 1738 cm^{-1} corresponded to the CH stretching of methyl groups ($–CH_3$) and to carbonyl (C═O) stretching of acetate group. The other peaks located at 1642, 1437, 1373, 1211, 1033 and 901 cm^{-1} are correlated to H-O-H bending of absorbed water, CH_2 bending, C-H bending vibration of CH_3 in the acetyl group, C–O stretching of acetyl group, C–O–C stretching of cellulose backbone and C-O-C stretching at β–(1 → 4) glycosidic linkage, respectively [56]. However, since that both samples contain about 30 wt % of plasticizer the interpretation of FT-IR spectra has been carried out by considering also the triacetin presence. Cellulose acetate and triacetin share the same main functional groups, so the presence of plasticizer in the samples must be detected mainly by the increasing of absorbance intensity of these functionality and by the slight shifting of the bands of acetate C-O stretching. Mixing generally enhances the alkoxyl groups of triacetin and cellulose acetate molecules [57]. The characteristic peaks of LDH were not observed in the ATR spectrum of CA-LDH. It happens when a small amount of filler is added to a sample [58]. For this reason, the spectra of CA and CA-LDH were perfectly stackable. After C, AD and AD + C processes, the decrease of absorbance bands at 1738, 1373,1211, 1033 and 901 cm^{-1} and the shift and broadening of hydroxyl group absorbance band (from 3483 to 3280 cm^{-1}) of both CA and CA-LDH samples clearly indicated the occurrence of different phenomena: plasticizer loss, deacetylation and regeneration of the hydroxyl functionalities and hydrogen bonding between the hydroxyl groups of cellulose molecules, and partial degradation of cellulose backbone. However, the interpretation of the first two phenomena has been complicated since the spectrum of plasticizer exhibited peaks which overlap with those of the cellulose acetate [59]. Usually, in fact, the triacetin loss is measured by the decreasing absorbance peaks at 1738 and 1211 cm^{-1} [46] and the deacetylation is followed by the decreasing and the increasing absorbance peaks at 1738 and 3483 cm^{-1}, respectively [50]. The degradation of cellulose backbone can be, instead, evaluated by the decreasing absorbance peaks at 1033 and 901 cm^{-1}. The spectra of CA and CA-LDH after C, AD and AD + C processes also showed an increase of peak absorbance at 1642 cm^{-1} due to water absorption from the samples during degradation processes and the formation of a new peak at 1550 cm^{-1} attributable to the presence of proteinaceous substances, probably due to bacterial activity [60]. The absence of an invariant peak in the FTIR patterns of both samples don't allow a quantitative analysis of the phenomena but only qualitative based on observing how the size of different peaks changes. The plasticizer loss was complete during all processes, as it highlighted from the TGA analysis, while from the observation of corresponding peaks the deacetylation and degradation was favored in AD and AD + C processes and from the presence of filler in anaerobic conditions confirming the results of disintegration tests and in according to Julinová et al. [61]. These authors reported that the degradation rate and the biodegradation percentage was strongly affected from degradation process type and filler type. In particular, they concluded that under anaerobic conditions, the samples biodegraded to the greatest extent with respect to composting in soil and that intercalation/exfoliation of inorganic fillers within the polymer matrix may have some importance on their biodegradation; in terms of the velocity of biodegradation, the use of non-dispersible fillers appeared to be a less appropriate solution, since biological degradation was only supported to a very limited extent compared with the intercalated fillers such as the LDH. The slight improvement of water barrier property of matrix due to the LDH presence, heighted from water absorption tests not reported for brevity, was instead responsible to the small difference of disintegration degree of CA and CA-LDH samples during C. Penetration of water and microorganisms into the matrix is limited, resulting in a reduced rate of disintegration of the CA-LDH sample.

4. Conclusions

This work investigated the full-scale biological degradation through dry anaerobic digestion and/or composting of two thermoplastic cellulose acetate-based bioplastics, in pure and composite forms. For both samples a disintegration of 50–37% was achieved during anaerobic digestion, while during composting the degradation did not exceed 20%. The disintegration obtained from the combined anaerobic digestion-composting process (58–40%) confirms how the main degradation occurred in anaerobic environment. Such disintegration was lower than that obtained previously at lab-scale on the same materials (74–55%). Despite this macroscopic degradation, the samples showed only minor superficial degradation as highlighted from SEM analysis where small fractures and exfoliation were detected in the anaerobically degraded samples. The biodegradation mechanism was determined by FT-IR spectroscopy, TGA and DSC analyses. The absence of a step in the TGA curves of degraded samples was the proof of the plasticizer loss from the cellulose acetate matrix during all treatments. The increase of T_g of degraded samples (from 115 to 127 to almost 200 °C) due to the deacetylation process was visible from DSC curves. All these aspects were confirmed by the decrease of absorbance bands of FT-IR spectra at 1738, 1373 and 1211 cm^{-1} and the shift and broadening of hydroxyl group absorbance band (from 3483 to 3280 cm^{-1}). The decreasing absorbance peaks at 1033 and 901 cm^{-1} also indicated a partial degradation of cellulose backbone.

Evidence shows discrepancies between results at different scales and suggests that it is not prudent to automatically extend results from the laboratory scale to the full scale. Another aspect not revealed on laboratory scale was that the biodegradation of the bioplastics involved mainly the plasticizer loss and deacetylation of the matrix with only a limited fragmentation of the cellulose backbone. It points out the weakness of the current industrial processes in the treatment of tested cellulosic bio-plastics, as contamination of the output (digestate/compost) by bioplastics fragments cannot be avoided. From these results emerged that important decisions are necessary for the management of full-scale treatment plants. Future experiments should primarily involve changes to the process scheme and/or its operating conditions. Higher thermophilic temperatures, longer residence times and bioplastics recirculation are probably necessary to increase the degradation of bioplastics at the end of the process.

The current study has only investigated the fate and the degradation of cellulose-based bioplastics waste within the biological process (anaerobic digestion and/or composting), not focusing on the responsible of such degradation but evaluating its degree. Consequentially, this study was not specifically designed to assess and identify the microorganisms involved in the cellulose acetate degradation, which will be further explored in future research.

Declaration of Competing Interest

The authors declare that they have no known competing financial interests or personal relationships that could have appeared to influence the work reported in this paper.

Data availability

Data will be made available on request.

Acknowledgment

The authors would like to thank the Biogas-und Kompostwerk Bützberg plant for their support in conducting the on-field tests. The project Prin 2017 “MultIFunctional poLymer cOmposites based on groWn matERials (MIFLOWER)” (grant number: 2017B7MMJ5_001) from the Italian Ministry of Education University and Research is kindly acknowledged. The Politecnico di Bari is also acknowledged for funding the project “Materials and energy recovery technologies by combined treatment of municipal solid waste and sewage sludge”.

Appendix A. Supplementary data

Supplementary data to this article can be found online at https://doi.org/10.1016/j.cej.2023.142301.

References

[1] European Parliament, Directive (EU) 2019/904 of the European Parliament and of the Council of 5 June 2019 on the reduction of the impact of certain plastic products on the environment, (2019) https://eur-lex.europa.eu/eli/dir/2019/904/oj.
[2] G. Fredi, A. Dorigato, Recycling of bioplastic waste: a review, Adv. Ind. Eng. Polym. Res. 4 (2021) 159–177, https://doi.org/10.1016/j.aiepr.2021.06.006.
[3] J.R.A. Pires, V.G.L. Souza, P. Fuciños, L. Pastrana, A.L. Fernando, Methodologies to assess the biodegradability of bio-based polymers—current knowledge and existing gaps, Polymers (Basel). 14 (2022) 1359, https://doi.org/10.3390/polym14071359.
[4] C. Rada, Ž. Stasiškien, J. Barbir, L. Draudvilien, Z.K. Chong, K. Kuchta, V. Voronova, W.L. Filho, Challenges and strategies for bio-based and biodegradable plastic waste management in europe, Sustain. 14 (2022) 16476, https://doi.org/10.3390/SU142416476.
[5] L. Dilkes-Hoffman, P. Ashworth, B. Laycock, S. Pratt, P. Lant, Public attitudes towards bioplastics – knowledge, perception and end-of-life management, Resour. Conserv. Recycl. 151 (2019), 104479, https://doi.org/10.1016/j.resconrec.2019.104479.
[6] European Bioplastics, Bioplastics Market Development Update 2022, (2022) https://www.european-bioplastics.org/market/.
[7] S. De Gisi, G. Gadaleta, G. Gorrasi, F.P. La Mantia, M. Notarnicola, A. Sorrentino, The role of (bio)degradability on the management of petrochemical and bio-based plastic waste, J. Environ. Manage. 310 (2022), 114769, https://doi.org/10.1016/j.jenvman.2022.114769.
[8] G. Gadaleta, S. De Gisi, F. Todaro, M. Notarnicola, Carbon footprint and total cost evaluation of different bio-plastics waste treatment strategies, Clean Technol. 4 (2022) 570–583, https://doi.org/10.3390/cleantechnol4020035.
[9] A. Folino, D. Pangallo, P.S. Calabrò, Assessing bioplastics biodegradability by standard and research methods: current trends and open issues, J. Environ. Chem. Eng. 11 (2023), 109424, https://doi.org/10.1016/j.jece.2023.109424.
[10] F. Bandini, E. Taskin, F. Vaccari, M. Soldano, S. Piccinini, A. Frache, S. Remelli, C. Menta, P. Sandro Cocconcelli, E. Puglisi, Anaerobic digestion and aerobic composting of rigid biopolymers in bio-waste treatment: fate and effects on the final compost, Bioresour. Technol. 351 (2022), 126934, https://doi.org/10.1016/j.biortech.2022.126934.
[11] G. Gadaleta, S. De Gisi, C. Picuno, J. Heerenklage, K. Kuchta, A. Sorrentino, M. Notarnicola, Energy recovery options for the management of cellulose-based bio-plastics and mixed municipal solid waste, Biomass and Bioenergy. 166 (2022), 106628, https://doi.org/10.1016/j.biombioe.2022.106628.
[12] M. Cucina, P. De Nisi, L. Trombino, F. Tambone, F. Adani, Degradation of bioplastics in organic waste by mesophilic anaerobic digestion, composting and soil incubation, Waste Manag. 134 (2021) 67–77, https://doi.org/10.1016/j.wasman.2021.08.016.
[13] G. Gadaleta, C. Ferrara, S. De Gisi, M. Notarnicola, G. De Feo, Life cycle assessment of end-of-life options for cellulose-based bioplastics when introduced into a municipal solid waste management system, Sci. Total Environ. (2023), 161958, https://doi.org/10.1016/j.scitotenv.2023.161958.
[14] H.N. Tran, N.B. Nguyen, N.H. Ly, S.W. Joo, Y. Vasseghian, Core-shell Au@ZIF-67-based pollutant monitoring of thiram and carbendazim pesticides, Environ. Pollut. 317 (2023), https://doi.org/10.1016/j.envpol.2022.120775.
[15] P.S. Tourinho, V. Kočí, S. Loureiro, C.A.M. van Gestel, Partitioning of chemical contaminants to microplastics: sorption mechanisms, environmental distribution and effects on toxicity and bioaccumulation, Environ. Pollut. 252 (2019) 1246–1256, https://doi.org/10.1016/j.envpol.2019.06.030.
[16] C. Jönsson, R. Wei, A. Biundo, J. Landberg, L. Schwarz Bour, F. Pezzotti, A. Toca, L. M. Jacques, U.T. Bornscheuer, P.O. Syrén, Biocatalysis in the recycling landscape for synthetic polymers and plastics towards circular textiles, ChemSusChem. 14 (2021) 4028–4040, https://doi.org/10.1002/cssc.202002666.
[17] S. Hyuk Lim, S.W. La, T. Thuy Hang Hoang, Q. Trung Le, S. Jang, J. Choo, Y. Vasseghian, S. Jun Son, S.W. Joo, Carbon capture and biocatalytic oxygen production of photosystem II from thylakoids and microalgae on nanobiomaterials, Bioresour. Technol. 368 (2023), 128279, https://doi.org/10.1016/j.biortech.2022.128279.
[18] S. Sohn, V.T. Huong, P.D. Nguyen, N.H. Ly, S. Jang, H. Lee, C. Lee, J. Il Lee, Y. Vasseghian, S.W. Joo, K.D. Zoh, Equilibria of semi-volatile isothiazolinones between air and glass surfaces measured by gas chromatography and Raman spectroscopy, Environ. Res. 218 (2023) 1–9, https://doi.org/10.1016/j.envres.2022.114908.
[19] A. Lee, M.S. Liew, Tertiary recycling of plastics waste: an analysis of feedstock, chemical and biological degradation methods, J. Mater. Cycles Waste Manag. 23 (2021) 32–43, https://doi.org/10.1007/s10163-020-01106-2.
[20] C. Medjili, N. Lakhdari, D. Lakhdari, A. Berchi, N. Osmani, I. Laourari, Y. Vasseghian, M. Berkani, Synthesis of novel PANI/PVA-NiCu composite material

for efficient removal of organic dyes, Chemosphere. 313 (2023), 137427, https://doi.org/10.1016/j.chemosphere.2022.137427.
[21] R. Prajapati, K. Kohli, S.K. Maity, B.K. Sharma, Potential chemicals from plastic wastes, Molecules. 26 (2021) 1–22, https://doi.org/10.3390/molecules26113175.
[22] J. Nikiema, Z. Asiedu, A review of the cost and effectiveness of solutions to address plastic pollution, Environ. Sci. Pollut. Res. 29 (2022) 24547–24573, https://doi.org/10.1007/s11356-021-18038-5.
[23] A. Folino, A. Karageorgiou, P.S. Calabrò, D. Komilis, Biodegradation of wasted bioplastics in natural and industrial environments: a review, Sustain. 12 (2020) 6030, https://doi.org/10.3390/su12156030.
[24] G. Gadaleta, S. De Gisi, C. Picuno, J. Heerenklage, L. Cafiero, M. Oliviero, M. Notarnicola, K. Kuchta, A. Sorrentino, The influence of bio-plastics for food packaging on combined anaerobic digestion and composting treatment of organic municipal waste, Waste Manag. 144 (2022) 87–97, https://doi.org/10.1016/j.wasman.2022.03.014.
[25] R. Altieri, M. Seggiani, A. Esposito, P. Cinelli, V. Stanzione, Thermoplastic blends based on poly(butylene succinate-co-adipate) and different collagen hydrolysates from tanning industry—ii: aerobic biodegradation in composting medium, J. Polym. Environ. 29 (2021) 3375–3388, https://doi.org/10.1007/s10924-021-02124-3.
[26] P. Intaraksa, Y. Rudeekit, P. Siriyota, T. Leejarkpai, Comparative study of the biodisintegration behavior of polylactic acid under laboratory and pilot-scale composting conditions, Adv. Mater. Res. 747 (2013) 678–681, https://doi.org/10.4028/www.scientific.net/AMR.747.678.
[27] G. Kale, R. Auras, S.P. Singh, R. Narayan, Biodegradability of polylactide bottles in real and simulated composting conditions, Polym. Test. (2007), https://doi.org/10.1016/j.polymertesting.2007.07.006.
[28] Z.K. Chong, A. Hofmann, M. Haye, S. Wilson, I. Sohoo, K. Kuchta, Lab-scale and on-field industrial composting of biodegradable plastic blends for packaging, Open Res. Eur. 2 (2022) 101, https://doi.org/10.12688/openreseurope.14893.1.
[29] H.S. Cho, H.S. Moon, M. Kim, K. Nam, J.Y. Kim, Biodegradability and biodegradation rate of poly(caprolactone)-starch blend and poly(butylene succinate) biodegradable polymer under aerobic and anaerobic environment, Waste Manag. 31 (2011) 475–480, https://doi.org/10.1016/j.wasman.2010.10.029.
[30] M. Cucina, G. Soggia, P. De Nisi, A. Giordano, F. Adani, Assessing the anaerobic degradability and the potential recovery of biomethane from different biodegradable bioplastics in a full-scale approach, Bioresour. Technol. 354 (2022), 127224, https://doi.org/10.1016/j.biortech.2022.127224.
[31] G. Viscusi, V. Bugatti, V. Vittoria, G. Gorrasi, Antimicrobial sorbate anchored to layered double hydroxide (LDH) nano-carrier employed as active coating on polypropylene (PP) packaging: application to bread stored at ambient temperature, Futur. Foods. 4 (2021), 100063, https://doi.org/10.1016/j.fufo.2021.100063.
[32] G. Gadaleta, S. De Gisi, M. Notarnicola, Feasibility analysis on the adoption of decentralized anaerobic co-digestion for the treatment of municipal organic waste with energy recovery in urban districts of metropolitan areas, Int. J. Environ. Res. Public Health. 18 (2021) 1–17, https://doi.org/10.3390/ijerph18041820.
[33] Stadtreinigung Hamburg, Stadtreinigung Hamburg - Natur pur - Biogas- und Kompostwerk Bützberg. https://www.stadtreinigung.hamburg/ueber-uns/muellverwertung-anlagen/biogas-und-kompostwerk-buetzberg/, (2018).
[34] EN ISO 16929:2021 Plastics — Determination of the degree of disintegration of plastic materials under defined composting conditions in a pilot-scale test, ISO: Geneva, Switzerland, 2021.
[35] D. Adamcová, M. Vaverková, Degradation of biodegradable/degradable plastics in municipal solid-waste landfill, Polish J. Environ, Stud, 2014.
[36] DIN 38414-2 - German standard methods for the examination of water, waste water and sludge; sludge and sediments (group S); determination of water content, of dry residue and of solids content (S 2), 1985.
[37] DIN 38409-1 - German standard methods for the examination of water, waste water and sludge; parameters characterizing effects and substances (group H); determination of total dry residue, filtrate dry residue and residue on ignition (H 1), 1987.
[38] DIN 38404-5 - German standard methods for examination of water, waste water and sludge; physical and physico-chemical characteristics (group C); determination of pH value (C5) | Engineering360, 1984.
[39] DIN 38404-8 - German standard methods for the examination of water, waste water and sludge; physical and physical-chemical parameters (group c); determination of the electrical conductivity, 1985.
[40] A. Kosheleva, G. Gadaleta, S. De Gisi, J. Heerenklage, C. Picuno, M. Notarnicola, K. Kuchta, A. Sorrentino, Co-digestion of food waste and cellulose-based bioplastic: from batch to semi-continuous scale investigation, Waste Manag. 156 (2023) 272–281, https://doi.org/10.1016/j.wasman.2022.11.031.
[41] G. Gadaleta, S. De Gisi, C. Picuno, J. Heerenklage, C. Di Iaconi, M. Notarnicola, K. Kuchta, A. Sorrentino, Effects of cellulose-based bio-plastics on the aerobic biological stabilization treatment of mixed municipal solid waste: a lab-scale assessment, J. Environ. Manage. 318 (2022), 115585, https://doi.org/10.1016/j.jenvman.2022.115585.
[42] M. Cucina, P. de Nisi, F. Tambone, F. Adani, The role of waste management in reducing bioplastics' leakage into the environment: a review, Bioresour. Technol. 337 (2021), 125459, https://doi.org/10.1016/j.biortech.2021.125459.
[43] H. Yagi, F. Ninomiya, M. Funabashi, M. Kunioka, Anaerobic biodegradation tests of poly(lactic acid) under mesophilic and thermophilic conditions using a new evaluation system for methane fermentation in anaerobic sludge, Int. J. Mol. Sci. 10 (2009) 3824–3835, https://doi.org/10.3390/ijms10093824.
[44] A.A. Marek, V. Verney, Photochemical reactivity of PLA at the vicinity of glass transition temperature. the photo-rheology method, Eur. Polym. J. 81 (2016) 239–246, https://doi.org/10.1016/j.eurpolymj.2016.06.016.
[45] A. Alassali, H. Moon, C. Picuno, R.S.A. Meyer, K. Kuchta, Assessment of polyethylene degradation after aging through anaerobic digestion and composting, Polym. Degrad. Stab. 158 (2018) 14–25, https://doi.org/10.1016/j.polymdegradstab.2018.10.014.
[46] J. Zhu, X. Li, C. Huang, L. Chen, L. Li, Structural changes and triacetin migration of starch acetate film contacting with distilled water as food simulant, Carbohydr. Polym. 104 (2014) 1–7, https://doi.org/10.1016/j.carbpol.2013.12.087.
[47] J. Zhu, X. Li, C. Huang, L. Chen, L. Li, Plasticization effect of triacetin on structure and properties of starch ester film, Carbohydr. Polym. 94 (2013) 874–881, https://doi.org/10.1016/j.carbpol.2013.02.020.
[48] N. Nomadolo, O.E. Dada, A. Swanepoel, T. Mokhena, S. Muniyasamy, A comparative study on the aerobic biodegradation of the biopolymer blends of poly(butylene succinate), poly(butylene adipate terephthalate) and poly(lactic acid), Polymers (Basel). 14 (2022) 1894, https://doi.org/10.3390/polym14091894.
[49] A. Samir, F.H. Ashour, A.A.A. Hakim, M. Bassyouni, Recent advances in biodegradable polymers for sustainable applications, Npj Mater. Degrad. 6 (2022) 68, https://doi.org/10.1038/s41529-022-00277-7.
[50] N. Yadav, M. Hakkarainen, Degradable or not? Cellulose acetate as a model for complicated interplay between structure, environment and degradation, Chemosphere 265 (2021), 128731, https://doi.org/10.1016/j.chemosphere.2020.128731.
[51] J. Puls, S.A. Wilson, D. Hölter, Degradation of cellulose acetate-based materials: a review, J. Polym. Environ. 19 (2011) 152–165, https://doi.org/10.1007/s10924-010-0258-0.
[52] A. Göpferich, Mechanisms of polymer degradation and erosion1, in: Biomater. Silver Jubil. Compend., Elsevier Science, 1996: pp. 117–128. https://doi.org/10.1016/B978-008045154-1.50016-2.
[53] A.A. Klyosov, Trends in biochemistry and enzymology of cellulose degradation, Biochemistry. 29 (1990) 10577–10585, https://doi.org/10.1021/bi00499a001.
[54] P. Basaran, Y.D. Hang, Purification and characterization of acetyl esterase from Candida guilliermondii, Lett. Appl. Microbiol. 30 (2000) 167–171, https://doi.org/10.1046/j.1472-765x.2000.00681.x.
[55] Y.S. Liu, J.O. Baker, Y. Zeng, M.E. Himmel, T. Haas, S.Y. Ding, Cellobiohydrolase hydrolyzes crystalline cellulose on hydrophobic faces, J. Biol. Chem. 286 (2011) 11195–11201, https://doi.org/10.1074/jbc.M110.216556.
[56] T. Sudiarti, D. Wahyuningrum, B. Bundjali, I. Made Arcana, Mechanical strength and ionic conductivity of polymer electrolyte membranes prepared from cellulose acetate-lithium perchlorate, IOP Conf, Ser. Mater. Sci. Eng. 223 (2017), 012052, https://doi.org/10.1088/1757-899X/223/1/012052.
[57] A.W. Cindradewi, R. Bandi, C.W. Park, J.S. Park, E.A. Lee, J.K. Kim, G.J. Kwon, S. Y. Han, S.H. Lee, Preparation and characterization of cellulose acetate film reinforced with cellulose nanofibril, Polymers (Basel). 13 (2021) 2990, https://doi.org/10.3390/polym13172990.
[58] F.J. Tommasini, L. da, C. Ferreira, L.G.P. Tienne, V. de, O. Aguiar, M.H.P. da Silva, L.F. da, M. Rocha, M. de, F.V. Marques, poly (methyl methacrylate)-sic nanocomposites prepared through in situ polymerization, Mater. Res. 21 (2018), https://doi.org/10.1590/1980-5373-mr-2018-0086.
[59] D. Littlejohn, R.A. Pethrick, A. Quye, J.M. Ballany, Investigation of the degradation of cellulose acetate museum artefacts, Polym. Degrad. Stab. 98 (2013) 416–424, https://doi.org/10.1016/j.polymdegradstab.2012.08.023.
[60] F. Ruggero, R. Gori, C. Lubello, Methodologies to assess biodegradation of bioplastics during aerobic composting and anaerobic digestion: a review, Waste Manag. Res. 37 (2019) 959–975, https://doi.org/10.1177/0734242X19854127.
[61] M. Julinová, L. Vaňharová, M. Jurča, A. Minařík, P. Duchek, J. Kavečková, D. Rouchalová, P. Skácelík, Effect of different fillers on the biodegradation rate of thermoplastic starch in water and soil environments, J. Polym. Environ. 28 (2020) 566–583, https://doi.org/10.1007/s10924-019-01624-7.